Available online at www.sciencedirect.com
ScienceDirect
Journal of the European Ceramic Society 28 (2008) 2075–2083
www.elsevier.com/locate/jeurceramsoc

Sintering and dielectric properties of $Cu_2Ta_4O_{12}$ ceramics

D. Szwagierczak *, J. Kulawik

Institute of Electron Technology, Cracow Division, Zabłocie 39, 30-701 Kraków, Poland

Received 22 May 2007; received in revised form 18 December 2007; accepted 4 January 2008
Available online 4 March 2008

Abstract

In this work, $Cu_2Ta_4O_{12}$ ceramic was investigated as a promising, lead-free, nonferroelectric material with high dielectric permittivity. The results of impedance spectroscopy studies carried out at frequencies 10 Hz to 2 MHz over a wide temperature range from −55 to 700 °C were analyzed in the impedance, dielectric permittivity and electric modulus formalisms. In complex impedance plots two distinct arcs were distinguished, ascribed to the semiconducting grains and to the insulating grain boundaries. $Cu_2Ta_4O_{12}$ ceramic was found to exhibit a high dielectric permittivity exceeding 10,000 at low frequencies in the temperature range 150–740 °C. High permittivity of this material was attributed to the formation of internal (grain boundary) barrier layer capacitors. The influence of sintering conditions on microstructure, composition and dielectric properties of $Cu_2Ta_4O_{12}$ ceramics was also studied.

Keywords: Sintering; Impedance spectroscopy; Dielectric properties; $Cu_2Ta_4O_{12}$ ceramic; Internal barrier layer capacitor; Capacitors

1. Introduction

Increasing demand for both environmentally benign materials and miniaturization of capacitive elements has resulted in growing interest in lead-free, perovskite-type, nonferroelectric compounds exhibiting the so-called giant dielectric phenomena. The best-known representative of this group of compounds is $CaCu_3Ti_4O_{12}$.[1–13] Much less attention has been paid to $Cu_2Ta_4O_{12}$ that exhibits similar dielectric characteristics and structure.[14–18]

Subramanian et al.[1] have studied the dielectric properties of 13 members of $ACu_3Ti_4O_{12}$ family of compounds. Among these, $CaCu_3Ti_4O_{12}$ (CCTO) shows the highest dielectric constant at 25 °C of approximately 10,000 at 100 kHz. High values exceeding 1600 were found also for $Sm_{2/3}Cu_3Ti_4O_{12}$, $Dy_{2/3}Cu_3Ti_4O_{12}$, $Y_{2/3}Cu_3Ti_4O_{12}$ and $Bi_{2/3}Cu_3Ti_4O_{12}$ ceramics. The neutron powder diffraction analysis of $CaCu_3Ti_4O_{12}$ has not revealed any indication of ferroelectric phase transition, the structure remaining cubic and centric down to −238 °C.

A very high and relatively temperature independent permittivity values of $CaCu_3Ti_4O_{12}$ over a wide temperature range was reported for ceramics,[1–8] crystals[9–12] and thin films.[12,13] Various models, both related to intrinsic[1,2] and extrinsic effects[3–13] were presented to explain this behavior. Extrinsic origin can be related to internal or surface barrier layer capacitance or electrode polarization. In the last few years, several authors indicated the Maxwell–Wagner-type polarization related to internal barrier layer capacitance (IBLC) effects as the most plausible origin of the giant dielectric constant of $CaCu_3Ti_4O_{12}$.

Sinclair et al.[3] stated on the basis of impedance spectroscopy studies that the very high dielectric permittivity of $CaCu_3Ti_4O_{12}$ ceramic is nonintrinsic and may be attributed to internal barrier layer capacitance related to heterogeneous microstructure, consisting of semiconducting grains and insulating grain boundaries. The semiconductor character of the grains may originate from small loss of oxygen during thermal treatment of the samples. As emphasized by these authors, in the case of $CaCu_3Ti_4O_{12}$ a possibility arises to obtain IBL capacitors as a result of a one-step firing in air at relatively low temperatures, below 1100 °C, whereas the fabrication of commercial IBLC based on $BaTiO_3$ or $SrTiO_3$ requires a complex, multistage process involving doping and treatment in reducing atmospheres.

In complex impedance plane plots of CCTO ceramics Shao et al.[4] found three distinct contributions ascribed to conducting domains and two types of insulating barriers—grain

* Corresponding author.
E-mail address: dszwagi@ite.waw.pl (D. Szwagierczak).

0955-2219/$ – see front matter © 2008 Elsevier Ltd. All rights reserved.
doi:10.1016/j.jeurceramsoc.2008.01.015

boundaries and domain boundaries in the descending frequency order, respectively. The insulating domain boundaries were attributed to ordered dislocations, while the insulating grain boundaries to the presence of reoxidized regions on the outer surfaces of semiconducting grains and to the segregation of a secondary CuO phase at grain boundaries.

Shri Prakash and Varma[5] stated the appearance of an additional low frequency semicircle in complex impedance plane plots of $CaCu_3Ti_4O_{12}$ ceramics sintered at higher temperatures. They ascribed this semicircle to the formation of a Cu-rich phase on sample surface and confirmed this by the fact of complete vanishing of this semicircle after removing the surface layer of the sample.

The impact of contact effects at the electrode/sample interfaces was studied for $CaCu_3Ti_4O_{12}$ ceramic by Yang et al.[6] They have proved experimentally that dielectric properties of the ceramic with high surface resistance ($>1.2 \times 10^8\ \Omega$ cm) were not influenced by both the sample thickness and the use of different types of metal electrodes (silver paint, evaporated Ag, sputtered Pt and evaporated Al). Also Shri Prakash and Varma[5] have observed no differences in impedance response of $CaCu_3Ti_4O_{12}$ pellets with different electrode materials, such as sputtered Au, Ag and Al.

As predicted theoretically and confirmed experimentally by X-ray photoelectron analysis by Zhang and Tang,[7] in CCTO lattice there coexist Ti^{3+} and Ti^{4+} ions. Due to the larger ionic radius of Ti^{3+} as compared with that of Ti^{4+}, formation of these first ions should result in lattice distortion and creation of polarons. Ti^{3+} and Ti^{4+} form Ti^{3+}–O–Ti^{4+} bonds, creating a linked path for conduction by polaron transport. Zhang and Tang showed that the variable range hopping (VRH) mechanism is responsible for bulk dc conductivity in CCTO ceramic.

Subramanian et al.[1] and Li et al.[11] stated that in the case of single crystals the large, temperature independent, low frequency dielectric constant of CCTO may be associated with the barrier layer mechanism due to twinning. Cohen et al.[9] suggested that it stems from spacial inhomogeneities of local dielectric response. Probable sources of these inhomogeneities may be: twin, compositional ordering or antiphase boundaries. Wu et al.[12] using transmission electron microscope proved the presence of numerous dislocations, regions with cation disorder and planar defects in the CCTO single crystals and indicated these structural defects as the cause of the development of barriers for electrical conductivity.

$CaCu_3Ti_4O_{12}$ shows an unusual structure in which a small cation Cu with a low coordination number occupies the A-site of perovskite structure. Strong tilting of TiO_6 octahedra results in rectangular four-fold coordination of Cu ions.[1]

$Cu_2Ta_4O_{12}$ has a structure similar to that of $CaCu_3Ti_4O_{12}$, with 50% vacancies in A-sites. X-ray diffraction studies of single crystals carried out by Vincent et al.[14] showed that $Cu_2Ta_4O_{12}$ exhibits orthorhombic pseudocubic structure and crystallizes in the space group *Pmmm*. The cell parameters determined for this compound are: $a = 7.5228$ Å, $b = 7.5248$ Å, and $c = 7.5199$ Å. The B-sites of the perovskite structure are occupied by Ta^{5+} cations (the mean Ta–O distance being 1.985 Å) and the A-sites—mainly by Cu^{2+} cations, the part of them remaining vacant. These authors also revealed the presence of Cu^{+} cations in some Cu^{2+} sites and determined the chemical formula of the studied crystal as $Cu_{1.03}Ta_2O_6$. In the crystal lattice of $Cu_2Ta_4O_{12}$ there occur three different Cu–O distances: 2.027, 2.763, and 3.293 Å.[14] The oxygen ions surrounding copper cations are arranged as three mutually perpendicular squares, thus leading to approximately four-fold coordination of Cu ions.

Ebbinghaus[15] has studied the influence of cooling speed on crystal structure, nonstoichiometry and magnetic behavior of polycrystalline $Cu_{2+x}Ta_4O_{12+\delta}$ samples calcined at 1025 °C for 25 h. These samples were found to exhibit a significant flexibility with respect to both the copper and oxygen contents. The synthesis of a 1:1 mixture of CuO and Ta_2O_5 resulted in the presence of residual tantalum oxide, revealed by XRD analysis. Single phase materials were obtained for the compositions with copper excess in the range $0.125 \leq x \leq 0.5$. No CuO or Cu_2O phases were detected even for the highest excess of copper ($x = 0.55$). It was stated that color, crystal structure and oxygen excess were dependent on the x value and cooling rate. The slowly cooled samples were green and changed their crystal structure from pseudotetragonal to pseudocubic for $x \geq 0.45$. The lattice parameters were $a = b = 7.5065$ Å and $c = 7.52229$ Å for $x = 0.125$, and $a = b = c = 7.5156$ Å for $x = 0.500$. The quenched samples were brown and showed cubic structure regardless of the copper content. For these samples the values of lattice constant increased linearly up to $a = 7.527$ Å with x increasing to 0.35. The oxygen excess δ grew linearly with the copper excess x for both the slowly cooled and the quenched $Cu_{2+x}Ta_4O_{12+\delta}$ samples and was significantly lower for the latter due to the presence of Cu^{+}.[15]

Renner et al.[16] have investigated dielectric behavior of single crystals of copper tantalum oxide in the broad frequency range up to 1 GHz at temperatures changing from −248 to 227 °C. Giant dielectric constant values found at low frequencies and/or at high temperatures were ascribed to surface barrier layer capacitors (SBLC) formation at the sample-electrode interface. Temperature dependence of dielectric constant exhibited a step-like transition from the low, intrinsic value of 100 to the giant values of 10^4–10^5 at higher temperatures. Almost constant level of dielectric permittivity was retained in the broad range of temperature. The step shifted towards higher temperatures with increasing frequency. At frequencies above 1 MHz high ε' values were not reached up to 227 °C. These authors suggested on the basis of ac and dc measurements that the intrinsic charge transport in $Cu_2Ta_4O_{12}$ was dominated by hopping conduction of Anderson-localized charge carriers.

Polycrystalline $Cu_2Ta_4O_{12}$ was synthesized by Ngoc et al.[18] from $(CuO)_x + Ta_2O_5$ ($x = 0.8$, 1, 1.2) by solid-state reaction in air at 1200 °C. A deficit of copper oxide during the synthesis was found to cause the appearance of Ta_2O_5 in the sample, whereas an excess of CuO gave a single phase compound. The samples were light green for $x = 0.8$, dark green for $x = 1$ and very dark for $x = 1.2$. It was stated that an excess of copper doping increases both ionic and electronic conductivities. The electronic conductivity of $Cu_2Ta_4O_{12}$ seems to be mainly of n-type.

The present work was focused on the relationship between sintering conditions and dielectric characteristics of $Cu_2Ta_4O_{12}$ ceramic. The second goal was impedance spectroscopy studies

in a wide temperature range aimed at getting insight into the origin of barrier layer capacitance behavior of this material.

2. Experimental

Synthesis of $Cu_2Ta_4O_{12}$ was carried out by a conventional solid-state reaction. The starting materials CuO and Ta_2O_5 were weighed in stoichiometric proportions, ball-milled in isopropyl alcohol, dried, pelletized and calcined at 1180 °C during 25 h. Then, the product was ball-milled, dried, mixed with water solution of polyvinyl alcohol, granulated and pressed into discs. After burnout of the organic binder, the samples were sintered in the temperature range 1200–1260 °C during 2–50 h. The pellets were placed on a platinum sheet during the firing process. The cooling rate was 200°/h. Phase compositions of the samples sintered in different conditions were analyzed by a Philips X'Pert diffractometer.

Silver electrodes were deposited on both sides of the ceramic pellets by screen printing and fired at 850 °C. Dielectric response of the samples was determined in complex dielectric permittivity ε^*, electric modulus M^* ($M^* = 1/\varepsilon^*$) and impedance Z^* formalisms in the wide temperature range from −55 to 740 °C as a function of frequency in the range 10 Hz to 2 MHz, using a LCR QuadTech meter. Dc resistivity of $Cu_2Ta_4O_{12}$ was measured in the temperature range 20–600 °C by means of a Philips resistance meter. Microstructure and elemental composition of the samples were investigated using FEI scanning electron microscope and EDAX Genesis microanalysis system.

3. Results and discussion

It was found that the color and density of $Cu_2Ta_4O_{12}$ samples after sintering were dependent on the applied firing procedure. The pellets sintered at 1200–1230 °C were light green, while those fired at higher temperatures and for longer times were dark green. It is well known that Cu^{2+} converts to Cu^+ at high temperatures (above 1030 °C in air). The change in sample color is presumably related to this reduction. The established optimal sintering conditions were 1220–1230 °C and 12–25 h. For lower sintering temperatures (1200–1220 °C) a longer sintering time up to 50 h was required to densify the samples. The values of relative density of the ceramics were found to increase with increasing sintering temperature and duration, e.g., were 72, 81 and 91% of the theoretical value (8.16 g/cm^3) for the samples sintered for 25 h at 1200, 1220 and 1250 °C, respectively.

X-ray diffraction analysis has shown that different sintering conditions resulted in differences in the phase compositions of the samples. The samples sintered at 1200–1230 °C for 25 h were single phase, while in those sintered at higher temperatures or for longer durations the presence of Ta_2O_3 or Ta_2O_5 was revealed. The appearance of these phases is most likely caused by a deficit of copper oxide originating from evaporation of CuO during the sintering process. CuO and Cu_2O secondary phases have not been detected, independently of the sintering temperature of the investigated samples.

The cell parameters calculated as a result of Rietveld refinement in cubic space group *Pm*-3, carried out for the samples sintered at 1200 and 1230 °C, were: $a = b = c = 7.51729$ Å and $a = b = c = 7.51825$ Å, respectively. The lattice parameter was slightly higher for the sample sintered at higher temperature. The a values determined in the present work are close to those obtained by Ebbinghaus[15] ($a = b = c = 7.5197$ Å) for $Cu_{2+x}Ta_4O_{12+\delta}$ quenched samples with a small copper excess ($x = 0.125$).

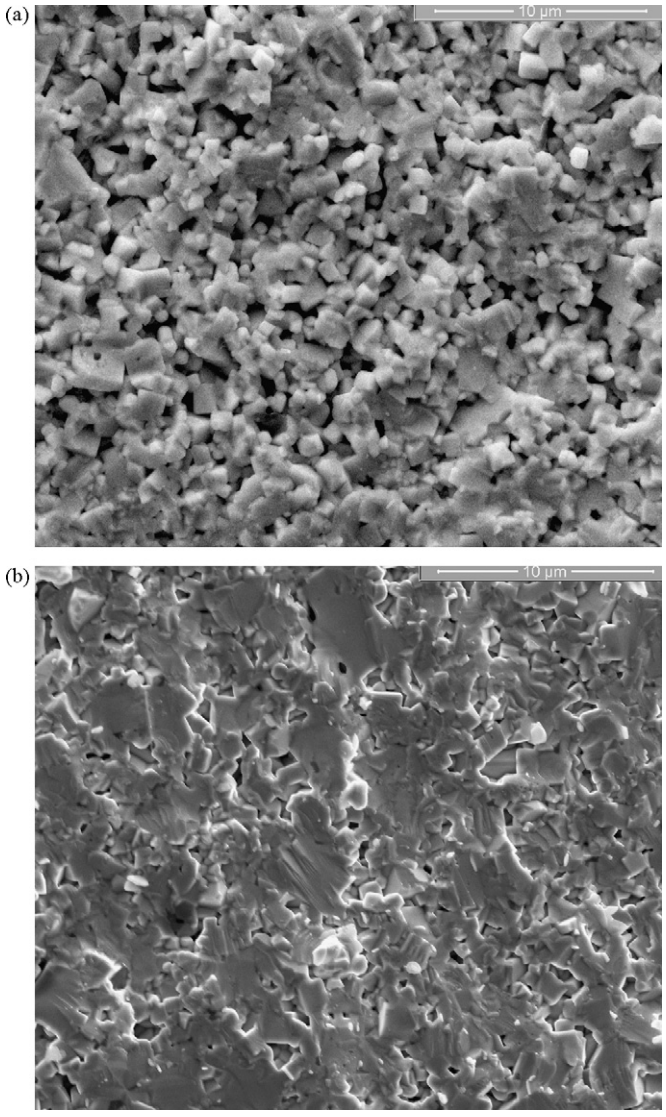

Fig. 1. SEM micrograph of the fractured cross-section of $Cu_2Ta_4O_{12}$ ceramic sintered at (a) 1220 °C (b) 1240 °C.

In Fig. 1 fractured cross-sections of the samples sintered at 1220 °C (a) and 1240 °C (b) are compared. The microstructure of the ceramics sintered at lower temperatures (1200–1220 °C) is fine-grained, with well-defined square shapes and almost uniform grain size of 0.5–3 μm (Fig. 1a). Increasing the sintering temperature to 1230–1260 °C has resulted in the development of irregular grain shapes and in a significant grain growth up to 5–7 μm (Fig. 1b). These differences between the morphologies of the samples after different thermal treatment are evident, but dissimilar and not so great as those reported for $CaCu_3Ti_4O_{12}$ by other authors.[4,5,8] For the Cu-stoichiometric and the Cu-

deficient CCTO ceramics sintered at high temperature (above 1050°C) discontinuous grain growth up to 50 μm, bimodal grain size distribution and the formation of a Cu-rich phase were observed by Shao et al.,[4] while Shri Prakash and Varma[5] have found a Cu-rich layer on the CCTO sample surface. In the present work, SEM observations and X-ray microanalysis did not reveal any large regions of Cu-rich phase neither in the surface layer nor around the grains. However, it was pointed out that Cu/Ta ratio is higher and oxygen content is lower for the samples fired at temperatures above 1230 °C. This confirms the enhanced reduction of Cu^{2+} ions into Cu^{+} at higher sintering temperatures. According to the XRD studies by Vincent et al.[14] and Ebbinghaus,[15] Cu^{+} ions may occupy Cu^{2+} sites in $Cu_2Ta_4O_{12}$ lattice.

Analysis of impedance spectroscopy data enables one to characterize the electrically different regions in a material under investigation. Ceramic materials can be usually well represented by the equivalent circuit consisting of a series connection of two parallel RC subcircuits, corresponding to grains and grain boundaries. In complex plane impedance plots these subcircuits are represented by two semicircular arcs.

Fig. 2 depicts in log–log coordinates the complex plane impedance plots in the whole temperature range studied for a $Cu_2Ta_4O_{12}$ sample sintered at1220 °C for 25 h. In Fig. 3a and b the relationship between imaginary and real parts of impedance is displayed for two selected temperatures from a lower and a higher temperature range, respectively. The arcs diminish and shift to the left with increasing temperature. $Z'' = f(Z')$ plots of the investigated ceramic samples in the temperature range 100–400 °C consist of one arc and a part of the second arc (Fig. 3a). The smaller, high frequency arc is related to grains, the part of the larger, low frequency one to grain boundaries. Below 100 °C, only the arcs attributed to grains are visible, whereas above 400 °C only those corresponding to grain boundaries.

As can be seen from Fig. 3b, at the highest investigated temperatures (above 500 °C), besides the semicircle with nonzero intercept with the real axis, ascribed to grain boundaries, an additional, small, low frequency arc occurs. This arc seems to be related to the microstructure, particularly to the grain sizes, because it almost disappears for the samples sintered at the lowest sintering temperature of 1200 °C. The third, slight, low frequency contribution to dielectric response may arise from electrode/sample contact effects, formation of a secondary phase layer on surface or, more likely, from the response of insulating boundaries of conducting domains. The existence of such domains, especially in larger grains originating from higher sintering temperature, was suggested for $CaCu_3Ti_4O_{12}$ ceramics by Shao et al.[4] These authors have found three contributions to dielectric response in complex impedance plane data and ascribed them to conducting domains, grain boundaries and domain boundaries. On the other hand, Shri Prakash and Varma[5] attributed an additional, low frequency arc to the formation of a Cu-rich phase on the sample surface. In the present work repolishing of the samples followed by their repeated measurements did not result in any remarkable decrease in permittivity; also, the additional, low frequency arc did not disappear. This indicates, along with approximately uniform composition and microstructure of the samples, that the formation of a Cu-rich blocking layer on the sample surface did not occur in the ceramics under investigation. Thus, the observed dielectric behavior could not be explained by the surface barrier layer capacitance mechanism.

The resistivities of grains R_g and grain boundaries R_{gb}, determined from the diameters of the arcs in the $Z'' = f(Z')$ plots (in the case of incomplete arcs the data were extrapolated), decrease with increasing temperature of measurement (in the

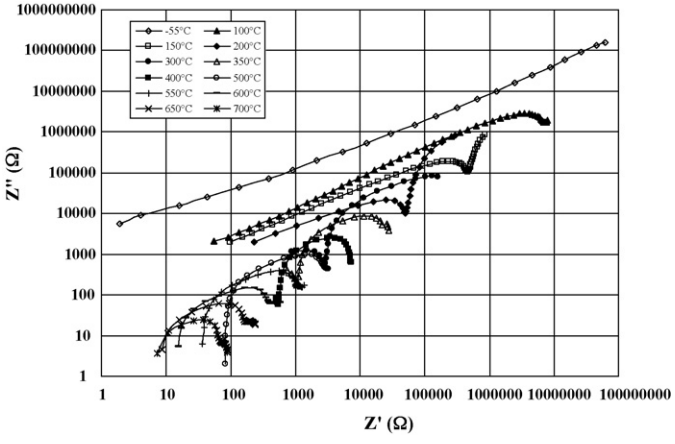

Fig. 2. $\log Z''$ versus $\log Z'$ plots for $Cu_2Ta_4O_{12}$ ceramic sintered at 1220 °C in the temperature range from −55 to 700 °C.

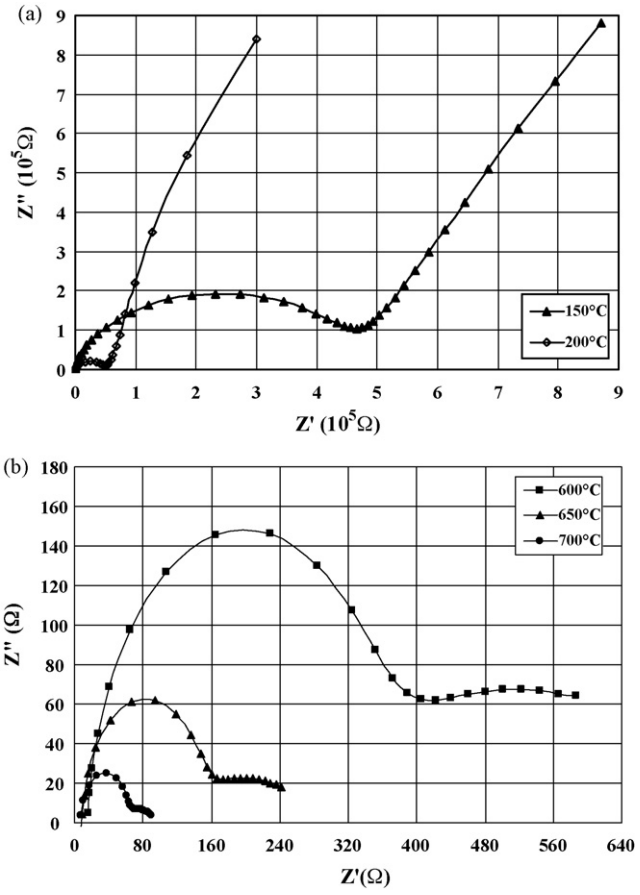

Fig. 3. Complex impedance plots for $Cu_2Ta_4O_{12}$ ceramic sintered at 1220 °C (a) at 150 and 200 °C (b) at 600, 650 and 700 °C.

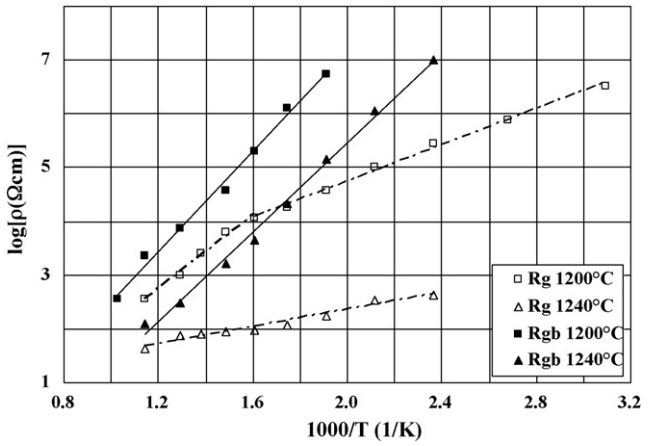

Fig. 4. Logarithm of resistivity of grains R_g and grain boundaries R_{gb} versus reciprocal temperature for $Cu_2Ta_4O_{12}$ ceramics sintered at 1200 and 1240 °C.

range 150–700 °C) from 10^4 to several Ω cm and from 10^7 to 10^2 Ω cm, respectively. In Fig. 4 resistances R_{gb} and R_g versus reciprocal temperature are compared for the samples sintered at 1200 and 1240 °C. The activation energies calculated from the slopes of Arrhenius plots are 0.93, 0.89 and 0.83 eV for the samples sintered at 1200, 1220 and 1240 °C, respectively. It was found that the resistances of grains R_g and grain boundaries R_{gb} decrease, whereas R_{gb}/R_g ratio grows with rising sintering temperature. The activation energies of grain resistances are lower (0.16–0.49 eV) and decrease more significantly with increasing sintering temperature than those of grain boundary resistances. Capacitances of grain boundaries C_{gb} and grains C_g were estimated from the relationship $2\pi f_{max}RC = 1$ (f_{max} – frequency corresponding to the maximum in impedance semicircle). C_{gb} values were established at the level of 15–35 nF. The estimated R_g values are 1–4 orders of magnitude lower than R_{gb}, whereas capacitances C_g are 2–3 orders lower than C_{gb}. Furthermore, the estimated capacitances of grain boundaries are almost constant, independently of sintering temperature.

In Fig. 5a and b, frequency dependencies of the real and imaginary parts of impedance are shown for several fixed temperatures. In $\log Z' = f(\log f)$ plots one or two steps separated by a region of dispersion are observed in the examined frequency range (Fig. 5a). Low frequency step becomes wider with increasing temperature. At temperatures below 150 °C, a strong frequency dependence of Z' occurs almost in the whole range of measurement. In the temperature range 300–550 °C low and high frequency steps are present. At temperatures exceeding 550 °C, Z' is frequency independent over a wide temperature range.

Three contributions to the dielectric response were found in the imaginary part of impedance spectra (Fig. 5b) attributed to grains, grain boundaries and domain boundaries in the descending frequency order. In the temperature range 150–400 °C, two maxima in $\log Z'' = f(\log f)$ curves are visible, related to grains and grain boundaries, while at lower temperatures only one distinct peak is detectable in the studied range, ascribed to grains. At the highest temperatures (above 550 °C), a distinct peak due to grain boundaries and an additional, low frequency, very flat

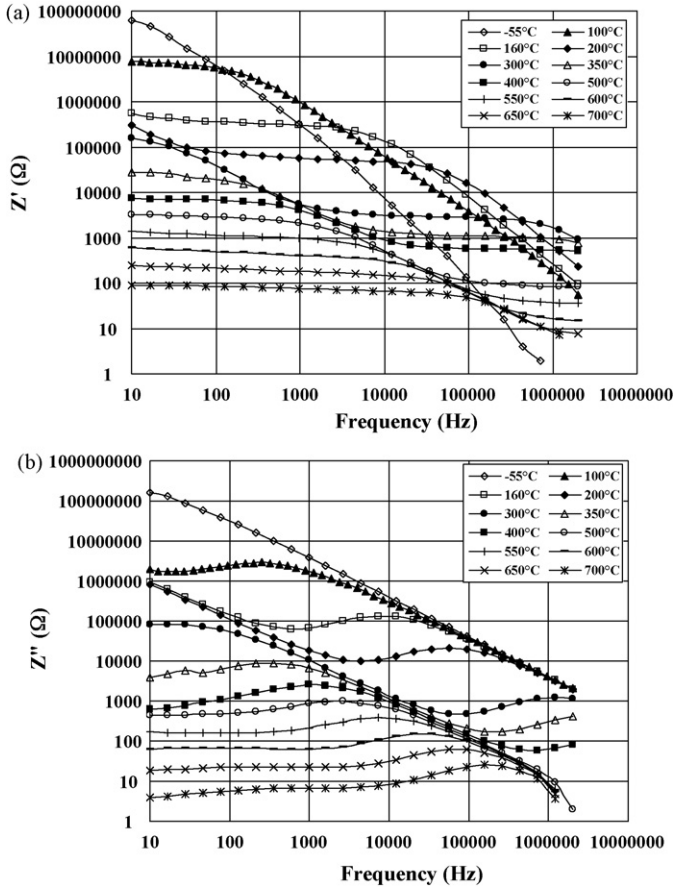

Fig. 5. Frequency dependence of impedance in the temperature range from −55 to 700 °C for $Cu_2Ta_4O_{12}$ ceramic sintered at 1220 °C (a) real part of impedance Z' (b) imaginary part of impedance Z''.

maximum, related most likely to the domain boundaries, can be distinguished. All maxima decrease and shift to higher frequencies with increasing temperature.

$Cu_2Ta_4O_{12}$ ceramic was found to exhibit a high dielectric permittivity, exceeding 10,000 at low frequencies in the temperature range 150–740 °C. In Fig. 6 the real part of permittivity is plotted against logarithm of frequency for a sample sintered

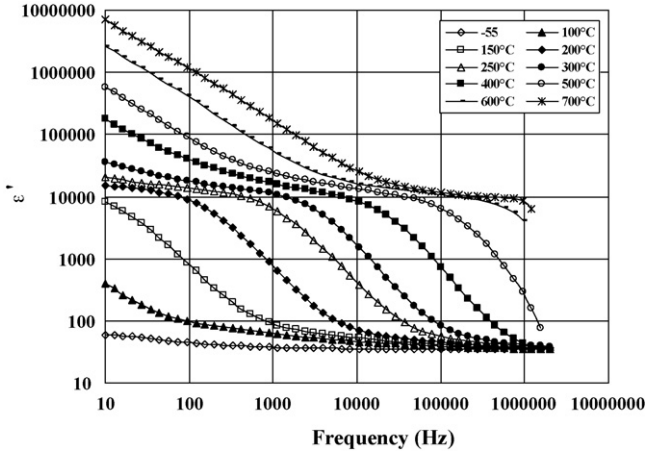

Fig. 6. Frequency dependence of the real part of permittivity for $Cu_2Ta_4O_{12}$ ceramic in the temperature range from −55 to 700 °C.

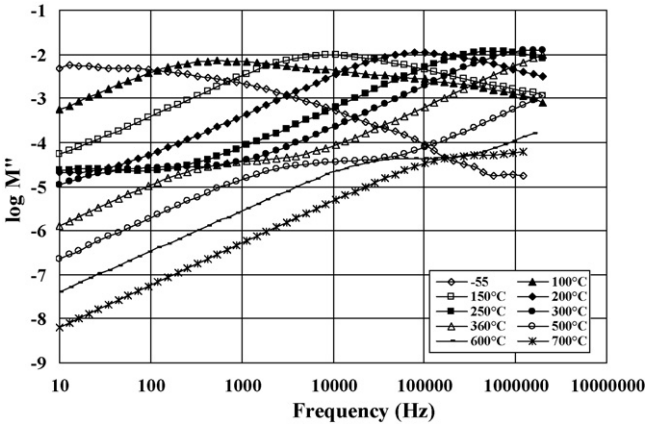

Fig. 7. Logarithm of the imaginary part of electric modulus as a function of frequency in the temperature range from −55 to 700 °C.

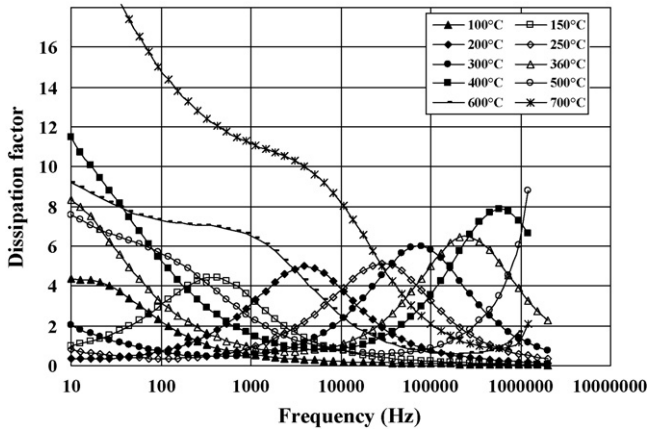

Fig. 8. Frequency dependence of dissipation factor in the temperature range from 100 to 700 °C for $Cu_2Ta_4O_{12}$ ceramic sintered at 1220 °C.

at 1220 °C. In the whole frequency range permittivity decreases with increasing frequency and the regions of flat and steep slopes of the plots occur one after the other. At lower temperatures, below 100 °C, ε' is almost frequency independent over a wide frequency range. In the temperature range 200–400 °C, low and high frequency plateaus, each converging at the same level for all temperatures, are followed by a region of permittivity dispersion. The low frequency step corresponds to ε' value of 10^4 and the high frequency one to the value of about 40. Both the steps shift to higher frequencies with increasing temperature. At higher temperature only one plateau at the level of 10^4 is detectable in the range of measurement.

As presented in Fig. 7 in log–log coordinates, in the plots of imaginary part of electric modulus M'' versus frequency two sets of peaks can be distinguished. The low-temperature, Debye-like relaxation maxima, which may be ascribed to the grains, are at the level of 10^{-2}. The second, high-temperature set of M'' peaks, observed above 250 °C and attributed to the grain boundaries, reaches 5×10^{-5}. The high frequency slopes of these peaks are significantly broadened, indicating the departure from the Debye relaxation behavior. The height of both types of peaks is almost temperature independent. Since the M'' peak values are proportional to reciprocal capacitances of grains and grain boundaries, respectively, this indicates that the capacitance of grains is approximately three orders of magnitude lower than that of grain boundaries, and both the C_g and the C_{gb} values are almost temperature independent.

In Fig. 8 frequency dependence of dissipation factor is shown with maxima shifting to higher frequencies with increasing temperature. As displayed in Fig. 9, the temperature dependence of relaxation times τ, estimated from the relationship $2\pi f_{Dmax}\tau = 1$ (where f_{Dmax} – frequency corresponding to dissipation factor maximum), obeys the Arrhenius law. The activation energy of dielectric relaxation determined from the slope of this plot is 0.75 eV. In Fig. 10, the real part of permittivity for a sample sintered at 1230 °C for 25 h is plotted as a function of temperature for six frequencies from the range 10 Hz to 1 MHz. Below 40 °C there occurs a region of low ε' values at the level ranging from tens for frequencies above 1 kHz to a few hundred for lower frequencies. Further temperature increase is associated with a

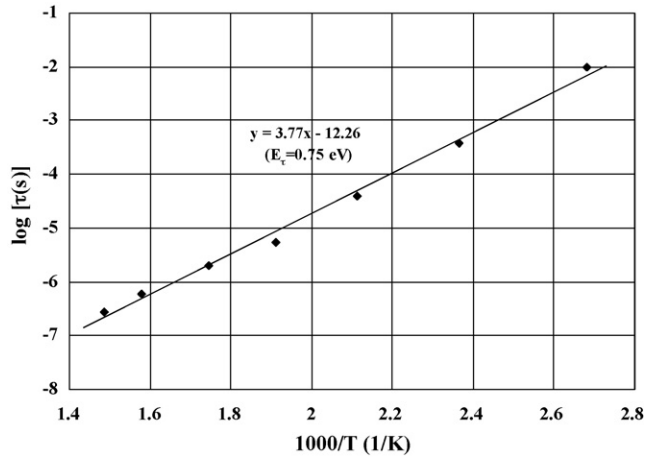

Fig. 9. Logarithm of relaxation times as a function of reciprocal temperature for $Cu_2Ta_4O_{12}$ ceramic sintered at 1220 °C.

rapid enhancement of permittivity to the level exceeding 10,000 for lower frequencies. In the temperature range 100–300 °C the slope of $\varepsilon' = f(T)$ is less steep, the location of this hump shifting towards higher temperatures with increasing frequency. How-

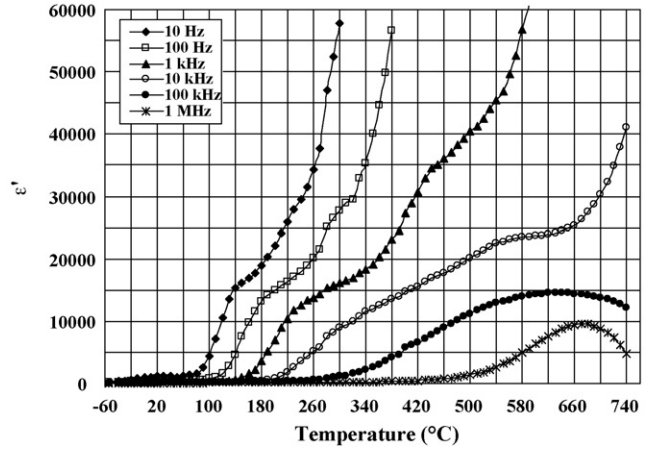

Fig. 10. Temperature dependence of the real part of permittivity for $Cu_2Ta_4O_{12}$ ceramic sintered at 1230 °C for 25 h.

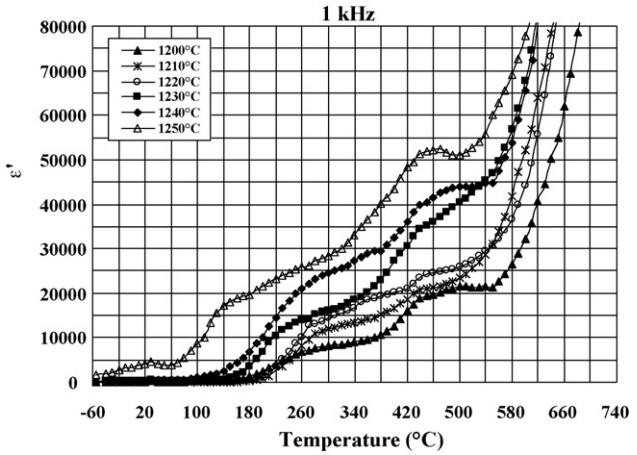

Fig. 11. Relationship between dielectric permittivity at 1 kHz and sintering temperature for $Cu_2Ta_4O_{12}$ ceramic fired at 1200–1250 °C for 25 h.

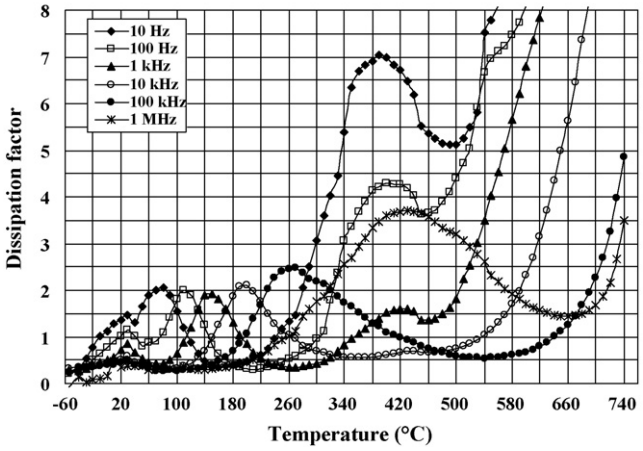

Fig. 13. Temperature dependence of dissipation factor for $Cu_2Ta_4O_{12}$ ceramics sintered at 1230 °C for 25 h, measured at 10 Hz to 1 MHz.

ever, the observed flattening of the permittivity curves was not so distinct as reported by other authors for $Cu_2Ta_4O_{12}$ crystals[16] and $CaCu_3Ti_4O_{12}$ ceramic and crystal samples.[1–4,8] For all the studied samples, the permittivities increase as temperature is raised almost in the whole examined range. A local maximum of permittivity, which occurs at 450–490 °C, disappears at higher frequencies, its position being frequency independent. The height of this peak or hump is giant (exceeding 10^6) at low frequencies and increases with decreasing frequency.

Both the ε' values and the shapes of permittivity versus temperature plots were found to change significantly with varying sintering conditions. The effect of sintering temperature is illustrated in Fig. 11 which compares $\varepsilon' = f(T)$ curves for the samples fired at different temperatures in the range 1200–1250 °C, for the measuring frequency of 1 kHz. A significant drop of ε' values with lowering sintering temperatures is observed. As shown in Fig. 12 for the samples sintered at 1230 °C during 6–50 h, the elongation of sintering time affects the courses of $\varepsilon' = f(T)$ curves in a similar way as the increase of sintering temperature does. The permittivity values are higher and the slopes of the plots steeper for longer sintering times.

Fig. 13 presents the dissipation factor versus temperature plots at 10 Hz to 1 MHz for a $Cu_2Ta_4O_{12}$ sample sintered at 1230 °C for 25 h. Broad maxima of $\tan\delta$ were observed, shifting towards higher temperatures with increasing frequency. The influence of the sintering temperature on the dissipation factor value is also evident. As depicted in Fig. 14 for frequency of 1 kHz, up to 200 °C the lowest $\tan\delta$ peaks are characteristic of the well-densified samples, obtained as a result of sintering at higher temperatures exceeding 1210 °C. The elongation of sintering time in the range 6–50 h results in a decrease of the dissipation factor at lower temperatures (up to 150 °C) and its increase at higher measuring temperatures.

In Fig. 15, the logarithm of dc electrical conductivity of $Cu_2Ta_4O_{12}$ ceramics sintered in different conditions is plotted as a function of reciprocal temperature. Generally, the conductivity increases with increasing sintering temperatures, especially those exceeding 1230 °C. However, at the lower temperature range of 20–120 °C the resistivity is almost temperature inde-

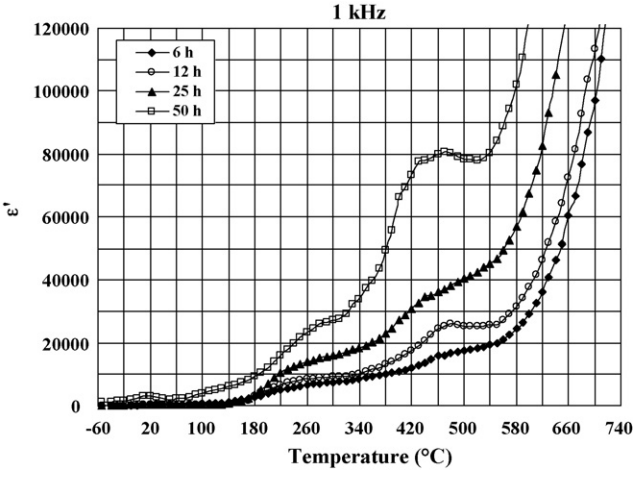

Fig. 12. Relationship between dielectric permittivity at 1 kHz and sintering time for $Cu_2Ta_4O_{12}$ ceramics fired at 1230 °C for 6–50 h.

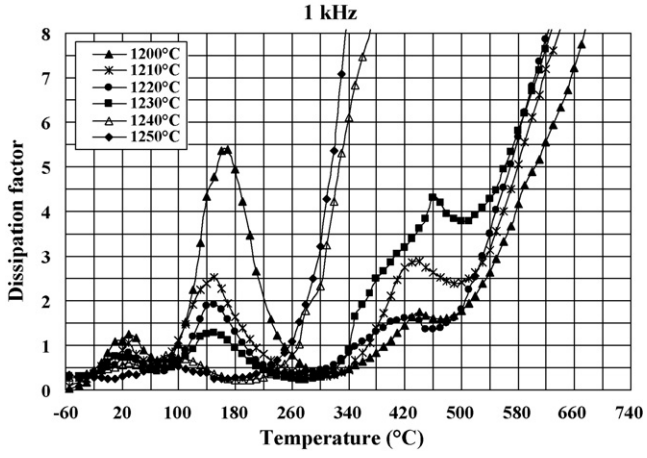

Fig. 14. Relationship between dissipation factor at 1 kHz and sintering temperature for $Cu_2Ta_4O_{12}$ ceramic fired at 1200–1250 °C for 25 h.

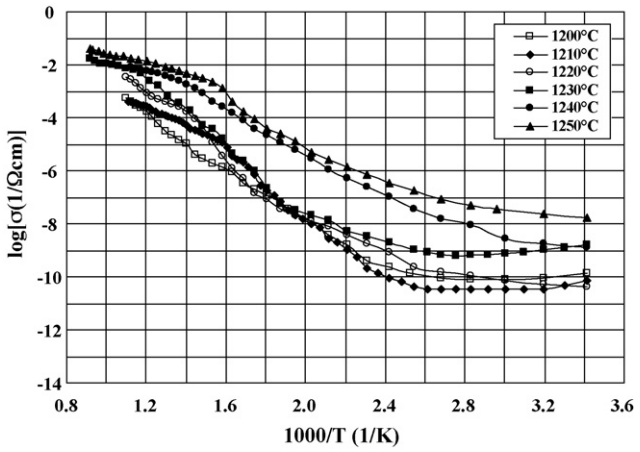

Fig. 15. Electrical conductivity as a function of reciprocal temperature in the range 20–600 °C for $Cu_2Ta_4O_{12}$ ceramic sintered at various temperatures.

pendent for all samples. Resistivity at 20 °C is relatively high, at the level of 10^8–10^{10} Ω cm. At higher temperatures semiconducting behavior is observed, characterized by the conductivities growing with increasing temperature. The activation energies of electrical conduction determined on the basis of the linear parts of Arrhenius plots were 0.7–1.2 eV in the temperature range 120–500 °C.

For internal (grain boundary) barrier layer capacitors, according to the Maxwell–Wagner model, for electrically heterogeneous ceramics with $R_{gb} \gg R_g$ and $C_{gb} \gg C_g$, the effective, static (low frequency) permittivity is expressed as:

$$\varepsilon'_s \approx \varepsilon_{gb} \frac{(d_g + d_{gb})}{d_{gb}}$$

where ε_{gb} – dielectric constant of the grain boundary layer; d_g – thickness of the grain; d_{gb} – thickness of the grain boundary.

It follows from this relationship that the growth of grain size visible in SEM images (Fig. 1) can be responsible for the observed increase in permittivity with increasing sintering temperature and duration. Another reason of the enhanced permittivity might be increasing tendency to reduction of Cu^{2+} into Cu^+ ions in grain interiors at higher sintering temperature, confirmed by X-ray microanalysis.

According to the investigations of other authors for similar compounds, like $CaCu_3Ti_4O_{12}$, and the results of the impedance spectroscopy and microstructure studies carried out in this work, we believe that the high permittivity values observed for $Cu_2Ta_4O_{12}$ ceramic samples, especially at low frequencies, arise from the spontaneous formation of internal barrier layer capacitors, composed of semiconducting grains and insulating grain boundaries. Small oxygen loss and partial reduction of Cu^{2+} to Cu^+ ions at high temperatures during sintering and reoxidation during cooling seems to be the main origin of the existence of semiconducting grains and more resistive barrier layers at the grain boundaries. Reoxidation of copper ions upon cooling is supposed to be confined to the region of grain boundaries (due to faster diffusion of oxygen along the grain boundaries than through the bulk), whereas the grain interiors still contain Cu^+ ions responsible for their enhanced electrical conductivity. Changes in the concentration of copper and oxygen vacancies, valence variations of Ta and Cu ions, dislocations or planar defects might be also the source of the IBLC mechanism. Further research, involving, e.g., annealing in an inert atmosphere, conductivity measurements as a function of partial oxygen pressure, determination of oxidation states of Cu and Ta, is needed for a better elucidation of the relationship between dielectric properties of $Cu_2Ta_4O_{12}$ ceramic samples and their processing conditions.

4. Conclusions

$Cu_2Ta_4O_{12}$ ceramics is a promising lead-free, high permittivity material. The advantageous high and relatively slightly changing with temperature permittivity is achieved for frequencies below 10 kHz and at elevated temperatures in the range 100–300 °C.

Complex impedance analysis of $Cu_2Ta_4O_{12}$ ceramics revealed the existence of two arcs attributed to semiconducting grains and insulating grain boundaries. The estimated resistances and capacitances of grains are 2–3 orders lower than those of grain boundaries. The enhanced permittivity of the samples sintered at higher temperatures may arise from the grain growth and an increase in differences between the resistivities of grains and grain boundaries. Unlike $CaCu_3Ti_4O_{12}$ ceramics, the segregation of a Cu-rich layer on the surface and abnormal grain growth were not observed in the investigated samples after thermal treatment at higher temperatures.

$Cu_2Ta_4O_{12}$ ceramics is supposed to be a spontaneously formed, one-step internal barrier layer capacitor. Such material could be a challenging alternative for the dominating IBLC capacitors based on $BaTiO_3$ or $SrTiO_3$, requiring doping and sophisticated, multistage processing.

Acknowledgement

This work has been supported by Polish Ministry of Science and Higher Education under Grant No. N507037 31/0906.

References

1. Subramanian, M. A., Li, D., Duan, N., Reisner, B. A. and Sleight, A. W., High dielectric constant in $ACu_3Ti_4O_{12}$ and $ACu_3Ti_3FeO_{12}$ phases. *J. Solid State Chem.*, 2000, **151**, 323–325.
2. Ramirez, A. P., Subramanian, M. A., Gardel, M., Blumberg, G., Li, D., Vogt, T. *et al.*, Giant dielectric constant response in a copper-titanate. *Solid State Commun.*, 2000, **115**, 217–220.
3. Sinclair, D. C., Adams, T. B., Morrison, F. D. and West, A. R., $CaCu_3Ti_4O_{12}$: one-step internal barrier layer capacitor. *Appl. Phys. Lett.*, 2002, **80**, 2153–2155.
4. Shao, S. F., Zhang, J. L., Zheng, P. and Wang, C. L., Effect of Cu-stoichiometry on the dielectric and electric properties in $CaCu_3Ti_4O_{12}$ ceramics. *Solid State Commun.*, 2007, **142**, 281–286.
5. Shri Prakash, B. and Varma, K. B. R., The influence of the segregation of Cu-rich phase on the microstructural and impedance characteristics of $CaCu_3Ti_4O_{12}$ ceramics. *J. Mater. Sci.*, 2007, **42**, 7467–7477.
6. Yang, J., Shen, M. and Fang, L., The electrode/sample contact effects on the dielectric properties of the $CaCu_3Ti_4O_{12}$ ceramic. *Mater. Lett.*, 2005, **59**, 3990–3993.

7. Zhang, L. and Tang, Z.-J., Polaron relation and variable-range-hopping conductivity in the giant-dielectric-constant material $CaCu_3Ti_4O_{12}$. *Phys. Rev. B*, 2004, **70**, 174306.
8. Ni, L., Chen, X. M., Liu, X. Q. and Hou, R. Z., Microstructure-dependent giant dielectric response in $CaCu_3Ti_4O_{12}$ ceramics. *Solid State Commun.*, 2006, **139**, 45–50.
9. Cohen, M. H., Neaton, J. B., He, L. and Vanderbilt, D., Extrinsic models for the dielectric response of $CaCu_3Ti_4O_{12}$. *J. Appl. Phys.*, 2003, **94**, 3299–3306.
10. Xe, L., Neaton, J. B., Cohen, M. H., Vanderbilt, D. and Homes, C. C., First-principles study of the structure and lattice dielectric response of $CaCu_3Ti_4O_{12}$. *Phys. Rev. B*, 2002, **65**, 214112.
11. Li, J., Sleight, A. W. and Subramanian, M. A., Evidence for internal resistive barriers in a crystal of the giant dielectric constant material: $CaCu_3Ti_4O_{12}$. *Solid State Commun.*, 2005, **135**, 260–262.
12. Wu, L., Zhu, Y., Park, S., Shapiro, S. and Shirane, G., Defect structure of the high-dielectric-constant perovskite $CaCu_3Ti_4O_{12}$. *Phys. Rev. B*, 2005, **71**, 014118.
13. Tselev, A., Brooks, C. M., Anlage, S. M., Zheng, H., Salamanca-Riba, L., Ramesh, R. *et al.*, Evidence for power-law frequency dependence of intrinsic dielectric response in the $CaCu_3Ti_4O_{12}$. *Phys. Rev. B*, 2004, **70**, 144101.
14. Vincent, H., Bochu, B., Aubert, J. J., Joubert, J. C. and Marezio, M., Crystal structure of $CuTa_2O_6$. *J. Solid State Chem.*, 1978, **24**, 245–253.
15. Ebbinghaus, S. G., Influence of composition and thermal treatment on the properties of $Cu_{2+x}Ta_4O_{12+\delta}$. *Progress Solid State Chem.*, 2007, **35**, 421–431.
16. Renner, B., Lunkenheimer, P., Schetter, M., Loidl, A., Reller, A. and Ebbinghaus, S. G., Dielectric behavior of copper tantalum oxide. *J. Appl. Phys.*, 2004, **96**, 4400–4404.
17. Heinrich, A., Renner, B., Lux, R., Reller, A. and Stritzker, B., Influence of oxygen pressure, temperature and substrate/target distance on $Cu_2Ta_4O_{12}$ thin films prepared by pulse-laser deposition. *Thin Solid Films*, 2005, **479**, 12–16.
18. Ngoc, H. N., Petitbon, F. and Fabry, P., Investigations on the mixed conductivity of copper tantalate. *Solid State Ion.*, 1996, **92**, 183–192.